Atomic harmonic generation in time-dependent *R*-matrix theory

A. C. Brown, D. J. Robinson, and H. W. van der Hart
Centre for Theoretical Atomic, Molecular and Optical Physics, Queen's University Belfast, Belfast BT7 1NN, United Kingdom

(Received 17 July 2012; published 28 November 2012)

We have developed the capability to determine accurate harmonic spectra for multielectron atoms within time-dependent *R*-matrix (TDRM) theory. Harmonic spectra can be calculated using the expectation value of the dipole length, velocity, or acceleration operator. We assess the calculation of the harmonic spectrum from He irradiated by 390-nm laser light with intensities up to 4×10^{14} W cm^{-2} using each form, including the influence of the multielectron basis used in the TDRM code. The spectra are consistent between the different forms, although the dipole acceleration calculation breaks down at lower harmonics. The results obtained from TDRM theory are compared with results from the HELIUM code, finding good quantitative agreement between the methods. We find that bases which include pseudostates give the best comparison with the HELIUM code, but models comprising only physical orbitals also produce accurate results.

DOI: 10.1103/PhysRevA.86.053420 PACS number(s): 32.80.Rm, 31.15.A−, 42.65.Ky

I. INTRODUCTION

In recent years, harmonic generation (HG) has become one of the richest veins of research for atomic, molecular, and optical physics. Not only has HG enabled ultrashort light-pulse generation [1], but it has also given rise to a series of very sensitive measurements of molecular [2], atomic, and even electronic dynamics [3]. The sensitive nature of HG has made it increasingly important to develop accurate methods of modeling the process.

Many studies aimed at describing HG make use of the single active electron (SAE) model [4,5], a significant simplification which allows for the efficient computation of harmonic spectra. SAE methods have been used to probe the relationship between atomic structure and HG. For instance, the Cooper minimum in argon has been linked with the minimum in the photoionization spectrum caused by a zero-dipole moment between the p ground-state wave function and the d wave function of the photoionized electron for a photon energy of around 48 eV [6,7]. The minimum is observed to exist in both the photoionization spectrum and the harmonic spectrum and is easily described by the SAE method as it does not depend on the interactions between different electrons. However, there have been various studies carried out in molecular systems where multielectron dynamics are found to be of great importance [2,8]. Even in atomic systems there are features of photoionization, and hence harmonic spectra that are the result of electronic interactions which require a multielectron description [3,9–11].

Over the last few years, we have developed time-dependent *R*-matrix (TDRM) theory to model the interaction of atoms with short, intense laser pulses, maintaining a full description of the multielectron dynamics involved [12–14]. TDRM has recently been extended to account for harmonic generation, and this capability was demonstrated in showing how autoionizing resonances can affect the harmonic spectrum of argon. The appearance of the autoionizing resonances in these spectra is a consequence of multielectron dynamics: the interference between the response of $3p$ and $3s$ electrons to the laser field [9]. These calculations represent an important shift in thinking on HG: the multielectron nature of the process is reflected in the theoretical approach, and while there are many processes that can be adequately described using SAE methods, there are many for which this more rigorous description may be required.

The determination of the harmonic spectrum can proceed through the calculation of the time-dependent expectation value of the dipole, dipole velocity, or dipole acceleration operator. At present there is discussion about which of these operators offers the best prediction of the harmonic response for a single atom. Recent work [15,16] has suggested that there is a natural connection with the dipole velocity, while, commonly, the dipole acceleration operator is used [17–19], especially for the description of high-order harmonics as better resolution can be obtained for the high-energy peaks [20]. Much early work in the field used the dipole length [21,22], and up until this point the description of HG in TDRM has been restricted to using this operator [9]. We note that the use of these various forms has been verified only within the SAE approximation, and hence we seek herein to verify the independence of HG with respect to the use of the dipole, its velocity, or acceleration in a multielectron system. We also assess which form offers the most numerically stable method, particularly when used with a limited multielectron basis set. Studies assessing the propagation of the wave function have demonstrated that to obtain the most accurate results for a limited basis in the TDRM approach the laser field is best described in the dipole length gauge [23]. On the other hand, time propagation in SAE calculations is commonly performed by describing the laser field in the velocity gauge. This difference indicates that we cannot necessarily rely upon knowledge gained from SAE calculations for the assessment of TDRM calculations.

We have extended the TDRM method to calculate the harmonic spectrum from the dipole velocity and acceleration operators simultaneously with the dipole operator spectrum. In this paper we cover the major theoretical aspects of this extension and apply the TDRM codes to He in a 390-nm laser field. Helium is chosen for three reasons. First, the simple structure allows for the systematic varying of the multielectron basis functions, the impact of which has been assessed for TDRM in terms of photoionization [23] but not for HG. Second, the absence of a closed core simplifies the calculation of dipole acceleration matrix elements, and hence we can compare spectra in all three forms. Finally, using He allows us to benchmark our approach against a proven alternative method: we compare our results with those obtained using the HELIUM code [24].

II. THEORY

A. TDRM theory

The TDRM approach is an *ab initio* nonperturbative theory for describing ultrafast atomic processes. Details of the method can be found in [12,23], so we only give a short overview here. The time-dependent Schrödinger equation for an atom containing $(N+1)$ electrons is

$$i\frac{\partial}{\partial t}\Psi(\mathbf{X}_{N+1},t) = H(t)\Psi(\mathbf{X}_{N+1},t). \tag{1}$$

The Hamiltonian H contains both the nonrelativistic Hamiltonian of the $(N+1)$-electron atom or ion in the absence of the laser field and the laser interaction term. The laser field is described using the dipole approximation in the length form and is assumed to be linearly polarized and spatially homogeneous. This form provides the most reliable ionization yields when only a limited amount of atomic structure is included [23].

We propagate a solution of the time-dependent Schrödinger equation Ψ on a discrete time scale with time step Δt in a Crank-Nicolson scheme. We can write the wave function at a time t_{q+1} in terms of the wave function at the previous time step t_q:

$$(H_m - E)\Psi_{t_{q+1}} = -(H_m + E)\Psi_{t_q}. \tag{2}$$

Here the imaginary energy E is defined as $2i/\Delta t$, and H_m is the Hamiltonian at the midpoint of the time interval, $t_{q+1/2}$.

In R-matrix theory, configuration space is partitioned into inner and outer regions. In the inner region, all electrons are within a distance a_{in} of the nucleus, and a full account is taken of all interactions between all electrons. In the outer region, an ionized electron moves beyond the boundary a_{in}, and thus exchange interactions between this electron and the electrons remaining close to the nucleus can be neglected. The ionized electron then moves in only the long-range multipole potential of the residual N-electron core and the laser field.

Following [13], we can evaluate Eq. (2) at the boundary a_{in} as a matrix equation:

$$\mathbf{F}(a_{\text{in}}) = \mathbf{R}(a_{\text{in}})\bar{\mathbf{F}}(a_{\text{in}}) + \mathbf{T}(a_{\text{in}}), \tag{3}$$

in which the wave function $\mathbf{F}$ at the boundary is described in terms of its derivative $\bar{\mathbf{F}}$ plus an inhomogeneous vector $\mathbf{T}$ arising from the right-hand side of Eq. (2). The R-matrix $\mathbf{R}$ connects the inner- and outer-region wave functions at the boundary a_{in}.

Given an inner-region wave function, $\mathbf{R}$ and $\mathbf{T}$ are evaluated at the boundary a_{in}. Subsequently, they are propagated outwards in space up to a boundary a_{out}, where it can be assumed that the wave function $\mathbf{F}$ has vanished. The wave function vector $\mathbf{F}$ is set to zero and then propagated inwards to the inner-region boundary. Once $\mathbf{F}$ has been determined at each boundary point, the full wave function can be extracted from the R-matrix equations. We can then iterate the procedure using Eq. (2).

B. Harmonic generation

The electric field produced by an accelerating charge is given, using the nonrelativistic Lienard-Wiechert potentials in the far-field limit, by

$$E(t) = k\left\langle \psi(t)\left|\frac{[p_z,H]}{i\hbar}\right|\psi(t)\right\rangle + keE_{\text{laser}}(t), \tag{4}$$

where e is the electronic charge, z is the laser polarization axis, k is a proportionality constant, p_z is the canonical momentum, and E_{laser} is the electric field of the laser pulse. We can write

$$\left\langle \psi(t)\left|\frac{[p_z,H]}{i\hbar}\right|\psi(t)\right\rangle = \frac{d}{dt}\langle\psi(t)|p_z|\psi(t)\rangle, \tag{5}$$

and it follows that

$$E(t) \propto \ddot{\mathbf{d}}(t) = \frac{d^2}{dt^2}\langle\psi(t)|\mathbf{z}|\psi(t)\rangle. \tag{6}$$

The power spectrum of the emitted radiation is then given, up to a proportionality constant, by $|\ddot{\mathbf{d}}(\omega)|^2$, the Fourier transform of $\ddot{\mathbf{d}}(t)$ squared.

Although the radiation produced is proportional to the dipole acceleration, it is common practice in HG calculations to calculate $\mathbf{d}(\omega)$, i.e., to use the expectation value of the dipole length instead. This is because a simple relationship exists between $\mathbf{d}$ and $\ddot{\mathbf{d}}$ which can be extended to include the dipole velocity form:

$$\omega^4|\mathbf{d}(\omega)|^2 = \omega^2|\dot{\mathbf{d}}(\omega)|^2 = |\ddot{\mathbf{d}}(\omega)|^2. \tag{7}$$

Therefore the harmonic response of a single atom can be expressed in terms of the expectation value of the dipole operator,

$$\mathbf{d}(t) = \langle\Psi(t)| - e\mathbf{z}|\Psi(t)\rangle, \tag{8}$$

or of its velocity,

$$\dot{\mathbf{d}}(t) = \frac{d}{dt}\langle\Psi(t)| - e\mathbf{z}|\Psi(t)\rangle, \tag{9}$$

or acceleration,

$$\ddot{\mathbf{d}}(t) = \frac{d^2}{dt^2}\langle\Psi(t)| - e\mathbf{z}|\Psi(t)\rangle, \tag{10}$$

where $\mathbf{z}$ is the total position operator along the laser polarization axis.

As discussed in [23] the TDRM code can use either the length or velocity gauge for the propagation of the wave function. While, in keeping with the findings of [23], we use the length gauge, we can still utilize the dipole velocity matrix elements produced by the R-matrix suite of codes which "seed" the TDRM code. Thus we can store both $\mathbf{z}$ and $d\mathbf{z}/dt$ and use Eqs. (8) and (9) directly for the determination of the time-varying expectation values of the dipole operator and the dipole velocity.

However, in order to calculate the expectation value of the dipole acceleration we cannot use Eq. (10) directly. Instead, using Ehrenfest's theorem, it is possible to write the dipole acceleration as

$$\ddot{\mathbf{d}}(t) = \left\langle\frac{\partial H}{\partial r}\right\rangle = \left\langle\frac{eZ\cos\theta}{\mathbf{r}\cdot\mathbf{r}}\right\rangle - eN_{\text{elec}}\langle\Psi|E(t)|\Psi\rangle, \tag{11}$$

where Z is the nuclear charge, $\mathbf{r}$ is the total position operator, θ is the angle between $\hat{\mathbf{r}}$ and $\hat{\mathbf{z}}$, and $N_{\rm elec}$ is the number of electrons. The second term in Eq. (11) is often seen without this factor of $N_{\rm elec}$ as in the SAE approximation it is just 1. We can make a small change to the way the radial integrals are calculated in the R-matrix suite, which allows the calculation of $\langle 1/\mathbf{r}\cdot\mathbf{r}\rangle$ instead of $\langle\mathbf{r}\rangle$. Then we can use Eq. (11) to calculate the dipole acceleration. Thus, we can now simultaneously calculate harmonic spectra using the dipole length, velocity, and acceleration operators. The propagation of the wave function is still carried out in the length gauge.

The use of the acceleration form will, however, be restricted to He-like targets. The use of Ehrenfest's theorem [in Eqs. (5) and (11)] requires that the wave function be exact, or close to it. For general multielectron systems we normally impose a fixed core where (at least) the first two electrons are restricted to a single orbital. Imposing this restriction means that the electronic repulsion is not fully described. More precisely, if the orbital of electron e_1 is fixed and the orbital of electron e_2 is not, then the action on e_2 will not necessarily equal minus the reaction on e_1. Thus, the commutator

$$\left[(\mathbf{p_1}+\mathbf{p_2}),\frac{1}{|\mathbf{r_1}-\mathbf{r_2}|}\right] \tag{12}$$

may not be guaranteed to vanish. On the other hand,

$$\left[(\mathbf{r_1}+\mathbf{r_2}),\frac{1}{|\mathbf{r_1}-\mathbf{r_2}|}\right] \tag{13}$$

will still vanish. Thus, while the expectation value $\langle[\mathbf{r}\cos\theta,H]\rangle$ can be calculated accurately, $\langle[[\mathbf{r}\cos\theta,H],H]\rangle$ cannot, rendering Ehrenfest's theorem untenable. Thus, the comparisons we employ for the simple He test case which follows can be extended to general multielectron systems only for the dipole length and velocity forms.

C. Calculation parameters

The one-electron basis used for describing the residual He^+ in the inner region consists of orbitals expressed in terms of B splines. The residual He^+ ion is represented through a series of models of increasing complexity [23]. The basic model consists of only the He^+ $1s$ state, which we call 1T (one true state). We also use two models comprising six states. The first is built using true orbitals $1s$, $2s$, $2p$, $3s$, $3p$, and $3d$ (6T) and the other using five pseudo-orbitals and the true $1s$ orbital: $1s,\bar{2}s,\bar{2}p,\bar{3}s,\bar{3}p$, and $\bar{3}d$, called 6P (six states with pseudostates). Pseudostate models have been found to be more accurate in the time propagation of the He wave function responding to short light fields, especially in the velocity-gauge description of the light field. Pseudostate models may thus provide a better basis for the description of the ionization and HG processes, provided that these processes are not affected by artificial resonances introduced by the pseudostates.

The inner-region radius is set at 20 a.u., which is sufficiently large to contain the residual ion for each model we use. The outer-region boundary is set at 600 a.u. to prevent any reflections of the wave function for the duration of the short laser pulse employed. The set of continuum orbitals contains 80 B splines for each angular momentum ℓ of the continuum electron up to a maximum value $L_{\rm max}=19$. Convergence testing was carried out retaining angular momenta up to a value of $L_{\rm max}=27$, and while changes in the harmonic spectra are observed, they occur at energies beyond the cutoff, outside the region of interest here. The outer region is divided into sectors of 2 a.u. containing 35 ninth-order B splines per channel. The time step used in the wave function propagation is 0.1 a.u.

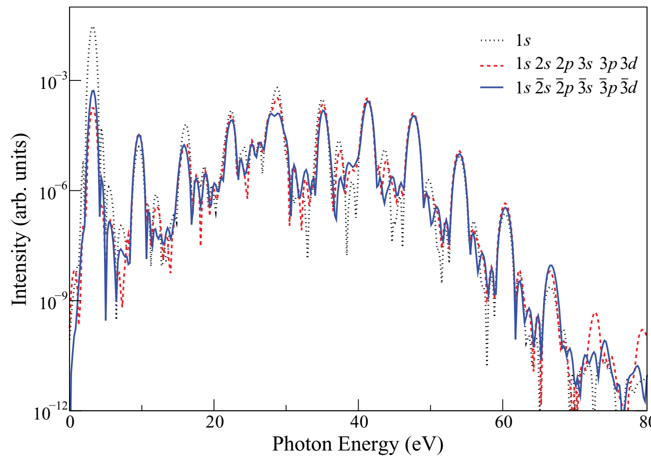

FIG. 1. (Color online) The harmonic spectrum (up to a constant of proportionality) as calculated from the dipole acceleration for He in a 390-nm, 4×10^{14} W cm^{-2}, 3-2-3 laser field, using as a model residual ion description, the $1s$ state (black dotted line), the $1s$, $2s$, $2p$, $3s$, $3p$, and $3d$ states (red dashed line), and the $1s,\bar{2}s,\bar{2}p,\bar{3}s,\bar{3}p$, and $\bar{3}d$ pseudostates (blue solid line). The single-state model provides a reasonable approximation to the more detailed descriptions beyond the first harmonic, where there is a large discrepancy between the spectra.

We use 390-nm laser pulses, consisting of a three-cycle $\sin^2$ ramp-on followed by two cycles at peak intensity, followed by a three-cycle $\sin^2$ ramp-off (3-2-3). We also calculate spectra for different pulse shapes and find that while the spectra change, the comparisons between them are generally described by the results presented below for the 3-2-3 pulse. There is one important exception to this general observation, which is discussed in Sec. III D.

III. RESULTS

A. Comparison of various target states

The harmonic response, as calculated from the expectation value of the dipole acceleration, of a He target in the 1T, 6T, and 6P configurations is shown in Fig. 1. The spectra display the expected form, a pronounced first-harmonic peak followed by a plateau of peaks at odd multiples of the fundamental photon energy, which decay exponentially beyond a cutoff. The cutoff of the plateau appears at a photon energy of approximately 45 eV. The standard formula for the cutoff energy, $I_p+3.2U_p$ [25], where I_p is the ionization potential and U_p is the ponderomotive energy, is not necessarily appropriate in this wavelength and intensity regime. Nevertheless, for the current parameters, it predicts a cutoff energy of 42 eV. The observed cutoff is therefore not inconsistent with the cutoff formula.

We can compare the spectra to assess how the description of atomic structure affects the calculated HG spectra. The 1T calculations are in better agreement with the more detailed

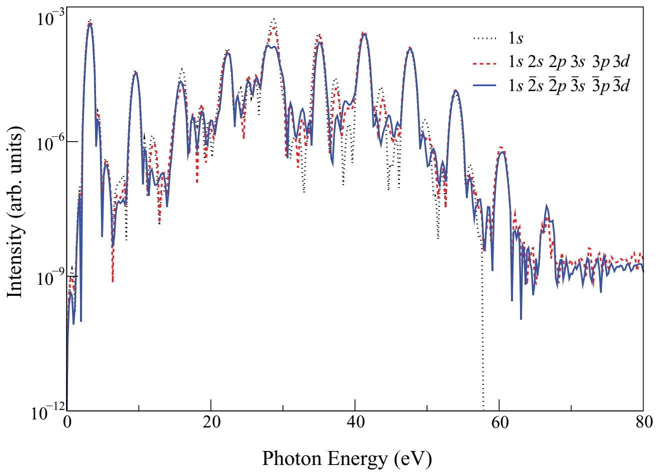

FIG. 2. (Color online) The length-form harmonic spectrum of He in a 390-nm, 4×10^{14} W cm^{-2}, 3-2-3 laser field, using as a residual ion description the 1T (black dotted line), 6T (red dashed line), and 6P (blue solid line) models (see Fig. 1 for details). Results from the 1T model provide a reasonable approximation to results from the more detailed descriptions, especially in the cutoff region. There is also good agreement for the first harmonic when compared with the large discrepancy in Fig. 1.

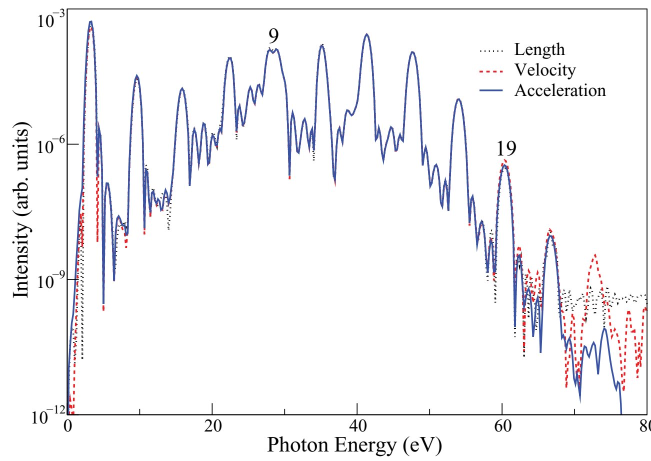

FIG. 3. (Color online) The harmonic spectrum of a pseudostate (6P) He target in a 390-nm, 4×10^{14} W cm^{-2}, 3-2-3 laser field, as calculated from the dipole length (black dotted line), velocity (red dashed line), and acceleration (blue solid line). Agreement to within 20% is found between all three spectra up to the 19th harmonic peak (60 eV). The spectra diverge beyond this point.

calculations at higher energies, especially in the cutoff region between the 13th and 19th harmonics, where agreement is within 30%. In the low-energy region, especially in the first harmonic, the spectra differ significantly; the first harmonic response in the 1T model is 60 times greater than that in the 6P model. The inconsistencies in the lower harmonics between the 1T and the 6T and 6P models imply that the low-energy harmonics in the dipole acceleration calculation are highly sensitive to changes in the atomic structure and that in the higher-energy cutoff region the details of the atomic structure are not as important. There is a factor of 3 difference in the first harmonic peak between the 6T and 6P models. As pseudostates may better represent the changes to the ground state than true states, this difference implies that the first harmonic is especially sensitive to the description of the ground state. The 6P spectrum shows a double-peak structure at the ninth harmonic stage which the two true-state models do not.

As the first term in the dipole acceleration is proportional to $1/r^2$, it is most sensitive to changes in the wave function at small r. If the description of the atomic structure close to the nucleus is not exact, this can lead to significant inaccuracies in the low-energy region of the spectra calculated from the dipole acceleration, especially the first harmonic peak. Figure 2 shows the same harmonic spectra as Fig. 1, but in this case the spectra are calculated from the dipole length operator. In this form the harmonics are far less sensitive to the details of the atomic structure close to the nucleus, as can be seen by the excellent agreement between the three spectra at the first and third harmonics (within 20%).

In fact the agreement between the spectra from the different target states is generally better in the length and velocity forms than in the acceleration: except for the 9th and 11th harmonics, the agreement between the 6T and 6P dipole-length spectra is within 20%. This further highlights that the dipole acceleration is especially sensitive to the description of atomic structure. The main difference between the three spectra appears again in the ninth harmonic. This difference is very similar to the difference seen in Fig. 1 in which the dipole acceleration was used to determine the harmonic spectrum. This indicates that this difference originates from the different bases used, rather than the choice of operator for the determination of the harmonic spectrum. This topic will be discussed further in Sec. III C.

B. Comparison of dipole length, dipole velocity, and dipole acceleration forms

As has been addressed in the previous section, TDRM theory can calculate harmonic spectra from the dipole length, dipole velocity, or dipole acceleration operators. We have already seen how the dipole acceleration is sensitive to the description of the atomic structure, particularly when it comes to the low-energy region of the spectrum.

Figure 3 shows the harmonic spectrum of 6P He in a 390-nm, 4×10^{14} W cm^{-2} laser field as calculated using the dipole length, velocity, and acceleration forms of the dipole matrix elements. The pseudostates model gives a more accurate description of the changes in the ground state due to the laser pulse and hence should give a more accurate picture of the harmonic spectrum than the true-state model. In terms of the agreement between the spectra this holds true, as the 6P model gives a consistent agreement between the three different approaches to calculate the harmonic spectrum where the 6T model breaks down at low harmonics. For the 6P model the three spectra agree within 20% at every harmonic peak up to the 19th harmonic, well into the cutoff region. In the 6T there is agreement within 20% between the dipole length and velocity spectra, but the dipole acceleration spectrum differs by 60%, 30%, and 40% in the first, third, and fifth harmonics, respectively.

Regardless of which model is used, the three spectra diverge beyond the 19th harmonic (Fig. 4), with the dipole length

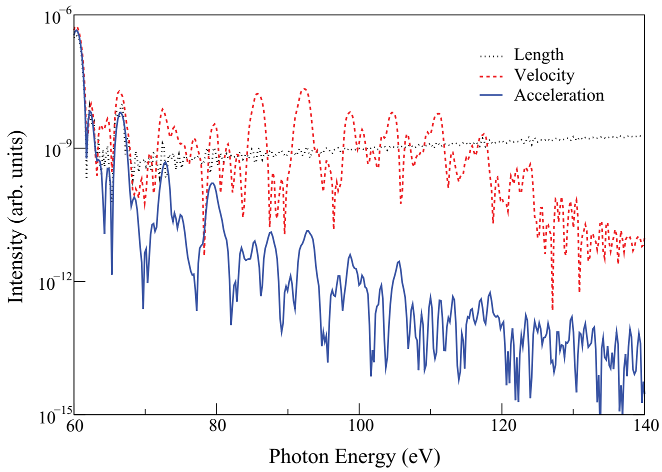

FIG. 4. (Color online) The high-energy harmonic spectrum of true state (6T) He target in a 390-nm, 4×10^{14} W cm^{-2}, 3-2-3 laser field, as calculated from the dipole length (black dotted line), velocity (red dashed line), and acceleration (blue solid line). The leftmost harmonic shown is the 19th harmonic, above which the spectra diverge.

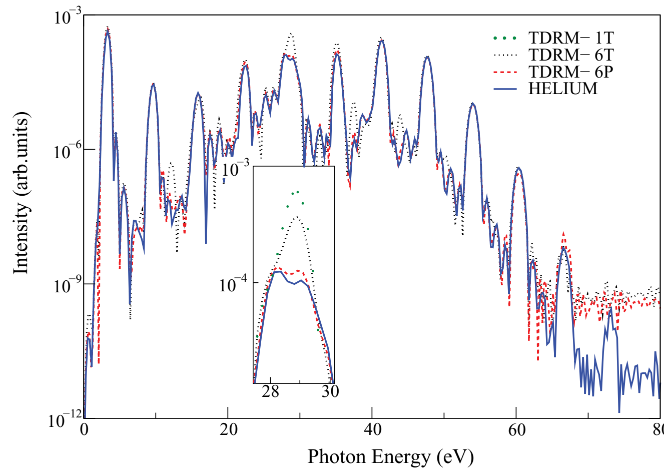

FIG. 5. (Color online) The harmonic spectra as calculated from the dipole length produced from the 6T (black dotted line) and 6P (red dashed line) He models for TDRM and from the HELIUM code (blue solid line). The 6P and 6T spectra agree with the HELIUM spectrum to within 20% and 30%, respectively, up to the 21st harmonic peak (except at the 9th and 11th harmonics for the 6T spectrum). The inset shows that both the 6P and HELIUM models have a structured peak at the 9th harmonic. The 1T (green circles) and 6T spectra do not.

spectrum becoming noisy and the dipole acceleration spectrum displaying a few more weak harmonics decaying into noise. The dipole velocity spectrum, on the other hand, displays a second plateau of peaks not seen in the other spectra. These peaks are not predicted classically, and their absence from the other spectra implies that they are spurious. This implies that the length and velocity forms are reliable, but only in an energy range up to and including the cutoff region. This is especially important as, for general multielectron targets, the acceleration form will be prohibitively sensitive to the limitations in the description atomic structure (see Sec. II C). However, by using both the dipole length and dipole velocity operators it is possible to obtain reliable harmonic spectra for multielectron systems using the TDRM approach.

C. Comparison with HELIUM

Having demonstrated that the TDRM method is self-consistent within a certain energy range, we now seek to benchmark our results against those from a proven alternative method. The HELIUM method [24] uses direct numerical integration of the full-dimensional TDSE to describe a two-electron system. By solving the TDSE directly, no significant approximations are made, and thus all important multielectron effects are included. This makes HELIUM an excellent code against which to benchmark TDRM.

Figure 5 shows the length-form harmonic spectra produced by the 6T and 6P models of He alongside that produced by the HELIUM code for a target in a 390-nm, 4×10^{14} W cm^{-2}, 3-2-3 laser field. At the harmonic peaks the agreement is very good. The 6P and HELIUM spectra agree to within 20% up to the 21st harmonics, while the 6T spectrum is within 30% except at the 9th and 11th harmonics

The inset in Fig. 5 shows the details of the ninth harmonic from the three calculations and the TDRM 1T model. The 6P model and HELIUM spectra show a structured peak which the 1T and 6T do not. The ponderomotive energy in the laser field shifts the He ground state down by around 5.7 eV, shifting the $1s3p$ bound state into the vicinity of the ninth harmonic peak. The presence of a bound state has been shown to give rise to such a structure in the harmonic peaks [9]. It is useful to notice that the 6T model may not describe the changes to the He$^+$ ground state in the laser field as accurately. Thus, the shift of the $1s3p$ state peak may differ, and consequently, we do not observe the double-peak structure in the ninth harmonic for the 6T spectrum. The 1T model does not account for any changes to the He$^+$ ground state, and differences between the 1T model and the other models are thus even larger. Expansion of the basis set in the TDRM approach thus leads to a harmonic spectrum which gets closer to the benchmark harmonic spectrum obtained using the HELIUM code.

The agreement for the TDRM velocity-form spectrum is even better: within 15% when comparing the velocity-form, 6P, TDRM spectrum with the length-form HELIUM spectrum. The excellent agreement between the spectra serves to give weight to the results obtained from both methods. The sensitivity of the harmonic spectra to the description of atomic structure makes it even more remarkable that the two methods overlap, especially in the low-energy region. Figure 6 shows the low-energy region of the velocity-form spectrum obtained from the 6P model TDRM code alongside the length-form spectra from the HELIUM code and from an SAE simplification derived from the HELIUM code [26]. The three spectra agree well in the first harmonic, whereas the acceleration-form spectra (not shown) vary widely. This confirms that the dipole velocity and length are significantly less sensitive to the description of atomic structure close to the nucleus and are probably more reliable in the low-energy, especially first-harmonic, region. The grid spacing in HELIUM and the limited basis set in TDRM impose constraints on the calculations very close to the nucleus. These

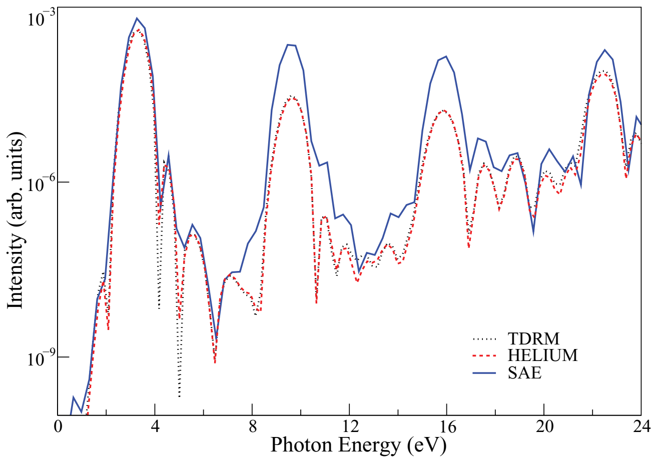

FIG. 6. (Color online) The low-energy region of the dipole velocity harmonic spectrum produced from the 6P He model in TDRM (black dotted line) and the length-form harmonic spectra from the HELIUM code (red dashed line) and its SAE derivative (blue solid line). The TDRM and HELIUM spectra are indistinguishable, but the SAE spectrum overestimates the harmonic spectrum at low energies.

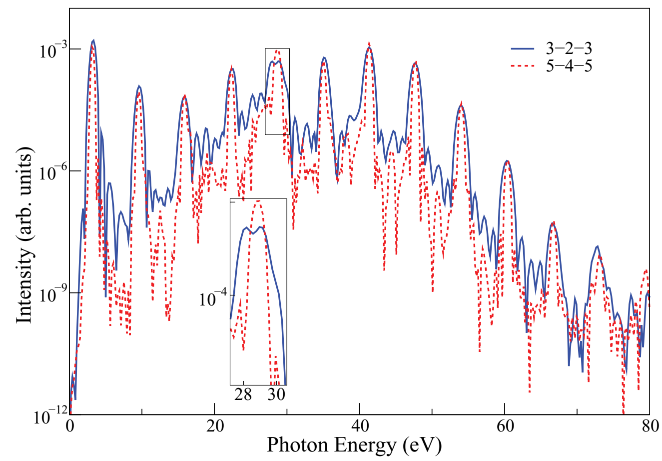

FIG. 7. (Color online) The dipole velocity harmonic spectra produced from the 6P He model for a 3-2-3 (blue solid line; three-cycle $\sin^2$ ramp-on, two-cycle peak intensity, three-cycle $\sin^2$ ramp-off) and a 5-4-5 pulse (red dashed line). Both pulses have a peak intensity of 4×10^{14} W cm^{-2} and a wavelength of 390-nm. The longer 5-4-5 pulse gives rise to narrower harmonic peaks, but the peak values are still within 20% of the 3-2-3 spectrum. The inset shows that there is a significant difference between the two spectra in the ninth harmonic.

constraints make it likely that the acceleration-form spectra are less reliable in the first harmonic, which could give rise to the discrepancy between the two methods.

In the third and fifth harmonics the SAE model markedly overestimates the harmonic spectra obtained from both the TDRM and HELIUM models, which are in excellent agreement with each other. This implies that the SAE model is not sufficient to describe low-energy harmonic spectra and that the lowest-energy harmonics are significantly more sensitive to atomic structure. We note that in the plateau and cutoff regions the SAE spectrum is in good agreement with the full HELIUM spectrum, lending justification to the use of the SAE approximation for investigating the generation of higher harmonics in He.

D. Comparison of various pulse lengths

To probe the effect of the laser pulse profile on the harmonic spectra, as well as the 3-2-3 (three-cycle $\sin^2$ ramp-on, two-cycle peak intensity, three-cycle $\sin^2$ ramp-off) profile, we ran calculations for various longer pulses, namely, 5-2-5, 3-4-3, and 5-4-5 pulses. Broadly speaking, while the spectra themselves change (with narrowing peaks for the longer pulses), the comparisons between the 1T, 6T, and 6P models with the HELIUM results or between the dipole length, velocity, and acceleration forms do not change significantly. Figure 7 shows the spectra produced by 3-2-3 and 5-4-5 laser pulses. The peak values do not change significantly with the different pulse profile, but the longer 5-4-5 pulse gives rise to narrower peaks and greater contrast. This gives a greater energy resolution between different peaks. Therefore the broad ninth harmonic peak in the 3-2-3 spectrum in Fig. 7 is further broadened by the presence of the nearby $1s3p$ bound state, whereas the narrower peak arising from the 5-4-5 pulse is isolated from any nearby atomic structure.

IV. CONCLUSIONS

We have extended the calculation of harmonic spectra in TDRM theory by determining these spectra through the time-varying expectation value of the dipole length, dipole velocity, and dipole acceleration operators and applied the adapted codes to He irradiated by a 390-nm, 4×10^{14} W cm^{-2} laser field. We have compared the spectra calculated using each form, assessed the effect of changing the multielectron basis set used to describe the residual ion, and benchmarked our results against those obtained from the HELIUM method.

We have shown that for harmonic photon energies up to and including the cutoff region the TDRM method provides results which are both self-consistent (between dipole length, velocity, and acceleration forms) and consistent with an independent approach. The favorable comparison between the TDRM and HELIUM methods in the velocity- and length-form spectra implies that the present approach can provide excellent results. Care must be taken in the lower harmonics, especially if using the dipole acceleration operator where the sensitivity to inaccuracies in the description of the atomic structure can seriously affect the reliability of the spectra obtained.

For general multielectron systems we can perform the calculations using both the dipole length and velocity, and we compare the two spectra in order to establish bounds on the reliability of the results. Both methods give excellent agreement for He well into the cutoff region. The divergence of the spectra beyond this occurs at energies which are usually outside the region of interest.

We have also probed the advantages of the various residual ion descriptions, which can be used within the TDRM method, finding that smaller basis sets, such as the 1T single-target state, provide an efficient way of testing the code and a reasonable approximation to the harmonic spectrum, but larger basis sets give more detailed spectra, as would be expected from their better description of the atomic structure involved. We also find that the inclusion of pseudostates in the He^+ basis seems to lead to more accurate harmonic spectra. This is particularly noticeable when compared with the highly accurate HELIUM method. This is largely due to the more precise way in which the pseudostate model describes the variations in the He^+ ground state in response to the laser field.

However, the use of pseudostates for general multielectron atoms can be problematic. By introducing nonphysical thresholds into the system, pseudoresonances can show up in the harmonic spectrum. These inadvertent features do not appear in the He case presented here, as the energies at which they become important are outside the harmonic region of interest. For general multielectron atoms, this is not necessarily the case. This does not mean that accurate calculations are not possible for larger atoms. Pseudostates can be used as long as care is taken: with knowledge of the position of pseudothresholds, unphysical resonances can be identified and disregarded. Second, although the 6T He model is not as close to the HELIUM spectrum as the 6P, it is still within 30% at every harmonic peak except the 9th and 11th harmonics (in the dipole length spectra). Physical orbitals can thus also be used to improve accuracy of harmonic spectra. The number of physical orbitals required may be larger than if pseudo-orbitals are used, but this is not a fundamental problem: it affects only the scale of the calculations. With careful analysis of, and comparison between, pure physical orbital and pseudostate models we can reliably assess the accuracy of harmonic spectra for general multielectron systems using TDRM theory.

Furthermore, even models which use only physical orbitals already offer significant gains over SAE models. A simple example of this is HG in Ar^+. Harmonics produced by Ar^+ ions have been suggested to be the source of the highest harmonics observed from a neutral Ar target [27,28]. The presence of three low-lying $3s^23p^4$ Ar^2+ thresholds can have a significant effect on the harmonic spectrum, and hence interactions between channels associated with these thresholds must be accounted for. These interactions are neglected in an SAE calculation but would be accounted for in a TDRM calculation involving purely physical orbitals.

We find that the reliability of the results is not significantly affected by the particular laser pulse profile used. We compared results for four different laser pulse profiles, finding that while the harmonic spectra differed between cases, the changes were consistent between the various target state models and with the HELIUM code results. In cases where atomic structure gives rise to structure in the harmonic spectrum the laser pulse length may affect the way in which this is observed. The greater energy resolution afforded by longer pulses can isolate the separate effects of atomic structure.

The results presented are also consistent with those from various peak intensities. We calculated harmonic spectra for intensities between 1×10^{14} and 4×10^{14} W cm^{-2}, finding that the results are largely consistent. At lower intensities the plateau region is severely truncated, so it is difficult to compare between the various spectra, but the agreement is still evident in the cutoff region.

The TDRM method has been rigorously tested up to intensities of 4×10^{14} W cm^{-2} and at wavelengths up to 390-nm but requires a significant amount of development to extend beyond these limits. It will be interesting to compare these findings with those that will be determined using the new R-matrix with time (RMT) codes [29,30], which may be better suited to address higher intensities and longer wavelengths. While the TDRM method has been proven to provide interesting insight into the multielectron nature of HG, it has thus far only been implemented for general multielectron atoms using the dipole length operator [9]. The next stage will be to apply TDRM at high intensities to systems other than He. While the dipole acceleration is too sensitive to the description of atomic structure to accurately describe such atoms, the length and velocity forms are stable enough to provide good results for general targets.

ACKNOWLEDGMENTS

A.C.B. and D.J.R. acknowledge support from the Department of Employment and Learning NI under the programme for government. H.W.H. is supported by the EPSRC under Grant Reference No. EP/G055416/1. The authors would like to thank Prof. K. T. Taylor and Dr. J. S. Parker for valuable discussions and assistance with the HELIUM code calculations.

[1] P. M. Paul, E. S. Toma, P. Breger, G. Mullot, F. Augé, P. Balcou, H. G. Muller, and P. Agostini, Science **292**, 1689 (2001).

[2] O. Smirnova, Y. Mairesse, S. Patchkovskii, N. Dudovich, D. Villeneuve, P. B. Corkum, and M. Y. Ivanov, Nature (London) **460**, 972 (2009).

[3] A. D. Shiner, B. E. Schmidt, C. Trallero-Herrero, H. J. Wörner, S. Patchkovskii, P. B. Corkum, J.-C. Kieffer, F. Légaré, and D. Villeneuve, Nat. Phys. **7**, 464 (2011).

[4] K. C. Kulander, K. J. Schafer, and J. L. Krause, *Atoms in Intense Radiation Fields*, edited by M. Gavrila (Academic, New York, 1992), pp. 247–300.

[5] K. J. Schafer and K. C. Kulander, Phys. Rev. Lett. **78**, 638 (1997).

[6] H. J. Wörner, H. Niikura, J. B. Bertrand, P. B. Corkum, and D. M. Villeneuve, Phys. Rev. Lett **102**, 103901 (2009).

[7] J. Higuet *et al.*, Phys. Rev. A **83**, 053401 (2011).

[8] P. B. Corkum, Phys. Today **64**(3), 36 (2011).

[9] A. C. Brown, S. Hutchinson, M. A. Lysaght, and H. W. van der Hart, Phys. Rev. Lett. **108**, 063006 (2012).

[10] A. Gordon, F. X. Kärtner, N. Rohringer, and R. Santra, Phys. Rev. Lett. **96**, 223902 (2006).

[11] S. Pabst, L. Greenman, D. A. Mazziotti, and R. Santra, Phys. Rev. A **85**, 023411 (2012).

[12] M. A. Lysaght, H. W. van der Hart, and P. G. Burke, Phys. Rev. A **79**, 053411 (2009).

[13] H. W. van der Hart, M. A. Lysaght, and P. G. Burke, Phys. Rev. A **76**, 043405 (2007).

[14] M. A. Lysaght, P. G. Burke, and H. W. van der Hart, Phys. Rev. Lett. **102**, 193001 (2009).

[15] J. C. Baggesen and L. B. Madsen, J. Phys. B **44**, 115601 (2011).
[16] D. J. Diestler, Phys. Rev. A **78**, 033814 (2008).
[17] J. H. Eberly and M. V. Fedorov, Phys. Rev. A **45**, 4706 (1992).
[18] D. G. Lappas, M. V. Fedorov, and J. H. Eberly, Phys. Rev. A **47**, 1327 (1993).
[19] K. Burnett, V. C. Reed, J. Cooper, and P. L. Knight, Phys. Rev. A **45**, 3347 (1992).
[20] T. F. Jiang and S.-I. Chu, Phys. Rev. A. **46**, 7322 (1992).
[21] J. H. Eberly, Q. Su, and J. Javanainen, Phys. Rev. Lett. **62**, 881 (1989).
[22] G. Bandarage, A. Maquet, T. Ménis, R. Taïeb, V. Véniard, and J. Cooper, Phys. Rev. A **46**, 380 (1992).
[23] S. Hutchinson, M. A. Lysaght, and H. W. van der Hart, J. Phys. B **43**, 095603 (2010).
[24] J. S. Parker, B. J. S. Doherty, K. T. Taylor, K. D. Schultz, C. I. Blaga, and L. F. DiMauro, Phys. Rev. Lett. **96**, 133001 (2006).
[25] J. L. Krause, K. J. Schafer, and K. C. Kulander, Phys. Rev. Lett. **68**, 3535 (1992).
[26] J. S. Parker, L. R. Moore, E. S. Smyth, and K. T. Taylor, J. Phys. B **33**, 1057 (2000).
[27] E. A. Gibson, A. Paul, N. Wagner, R. Tobey, S. Backus, I. P. Christov, M. M. Murnane, and H. C. Kapteyn, Phys. Rev. Lett. **92**, 033001 (2004).
[28] M. Zepf, B. Dromey, M. Landreman, P. Foster, and S. M. Hooker, Phys. Rev. Lett. **99**, 143901 (2007).
[29] L. R. Moore, M. A. Lysaght, L. A. A. Nikolopoulos, J. S. Parker, H. W. van der Hart, and K. T. Taylor, J. Mod. Opt. **58**, 1132 (2011).
[30] L. R. Moore, M. A. Lysaght, J. S. Parker, H. W. van der Hart, and K. T. Taylor, Phys. Rev. A **84**, 061404 (2011).